Coupling-reentrant phase transition, complex hysteretic behavior, and efficiency optimization in coupled phase oscillators submitted to colored flashing potentials

S. E. Mangioni* and R. R. Deza†
Departamento de Física, FCEyN, Universidad Nacional de Mar del Plata, Deán Funes 3350, 7600 Mar del Plata, Argentina

H. S. Wio‡
Centro Atómico Bariloche (CNEA) and Instituto Balseiro (CNEA and UNCuyo), 8400 San Carlos de Bariloche, Argentina
(Received 6 August 2002; published 21 November 2002)

A recent mean-field analysis of a model consisting of N nonlinear phase oscillators—under the joint influence of *global periodic* coupling with strength K_0 and of *local multiplicative* and additive noises—has shown a nonequilibrium phase transition towards a broken-symmetry phase exhibiting noise-induced transport, or ''ratchet'' behavior. In a previous paper we focused on the relationship between the character of the (mean velocity $\langle \dot{X} \rangle$ vs load force F) hysteresis loop, the number of ''homogeneous'' mean-field solutions, and the shape of the stationary mean-field probability distribution function (PDF). Here we assume that the multiplicative noises of the model are *Ornstein-Uhlenbeck* with common strength Q and self-correlation time τ. By resorting to an effective Markovian approximation, we study the τ dependence of the phase boundary, and that of the line signaling the transition from the ''interaction-driven regime'' to the ''noise-driven regime.'' We also study—for selected representative points of the K_0 vs Q phase diagram—the τ dependence of the transport properties induced by coupling and colored multiplicative noise (including the efficiency ε of the mechanical rectification process) and that of the above-mentioned PDF.

DOI: 10.1103/PhysRevE.66.051106 PACS number(s): 05.40.−a, 87.10.+e, 82.40.Bj

I. INTRODUCTION

Evidence accumulated mainly over the last 3 decades has radically changed our traditional concept of noise as a nuisance. A vast collection of phenomena that seem to be generic in far-from-equilibrium situations teaches us that fluctuations can also play a *constructive* role. A partial list of such phenomena includes noise-induced unimodal-bimodal transitions in some zero-dimensional models (describing either concentrated systems or uniform fields) [1], shifts in critical points [2], stochastic resonance in zero-dimensional and extended systems [3,4], noise-delayed decay of unstable states [5], noise-induced spatial patterns [6], etc. A Langevin description of the systems exhibiting such phenomena reveals common aspects among most of them: on one hand, the intrinsic dynamics is nonlinear; on the other, fluctuations usually act *multiplicatively* on the system, i.e., their representative variables appear in the corresponding Langevin equations multiplying (usually nonlinear) functions of the system's variables. In this paper we shall focus on two other phenomena in the same class as the aforementioned collection: noise-induced *phase* transitions in extended systems [6,7], and noise-driven *transport* (''Brownian motors'' or ''ratchets'' [8], nicely discussed by Feynman [9] and inspiring the present development of a ''nanomechanics'' that radically departs from the principles upon which macroscopic machines are built [10]).

For the sake of mathematical simplicity, multiplicative noises are usually modeled as white. This implies *excluding from the outset* time scales that are much shorter than the ''deterministic'' (i.e., coarse-grained) ones of the system they couple to, and *assuming* at the same time that the typical correlation time of the fluctuations is still well below this cutoff time scale. We should keep in mind, however, that a multiplicative noise is nonetheless but an effective model for the action of an external source that exchanges energy with the system in a far-from-equilibrium regime, and has its own characteristic time scales (not always negligible with respect to those of the system). In most cases, the above assumption is too simplistic, since the self-correlation time τ of fluctuations coupled multiplicatively to the system—although short compared with the deterministic time scales—is measurable and non-negligible [1,11–14]. Thus motivated (and aware of the nontrivial effects produced by colored noise in zero-dimensional models, such as the reentrance as a function of τ found in Ref. [15]) in Refs. [16] we have explored—in the mean-field approximation (MFA)—the consequences of letting the multiplicative noises in the model of Refs. [7]) have a *finite* τ.

In Ref. [17] a ratchetlike transport mechanism was shown to arise—through a symmetry-breaking nonequilibrium phase transition—in a system of nonlinear phase oscillators that interact through *periodic* forces, while being submitted to *multiplicative* white noises (as well as additive or thermal ones) and deterministic external forces. The latter, as well as the functions to which the multiplicative noises couple, can be derived from *symmetric* periodic potentials. The nonequilibrium phase transition—jointly induced by the coupling and the multiplicative noises—is *reentrant* as the latter become too strong. Among the most prominent novel features found by the authors in Ref. [17] through a strong-coupling

*Electronic address: smangio@mdp.edu.ar
†Electronic address: deza@mdp.edu.ar
‡Electronic address: wio@cab.cnea.gov.ar

analysis, we may cite *negative mobility* just outside the left phase boundary, and *anomalous hysteresis* inside it. In Ref. [18] we performed a mean-field analysis of the whole ordered phase and found a transition in the character of the hysteresis cycle, which is in turn intimately associated to the number of a certain kind of solutions to the mean-field equations, and with the shape of the stationary probability distribution.

As in Refs. [16], in this paper we study the effects of a nonzero self-correlation time τ (color) of the multiplicative noises, using a mean-field scheme. Our main findings are (1) the transition becomes *reentrant* as a function of K_0 (for $\tau \neq 0$, ordering is possible only *below* certain critical coupling); (2) for large enough τ, the response of the particle current $\langle \dot{X} \rangle$ to the load force F becomes very complex; (3) the efficiency ε of the mechanical rectification process shows a strong dependence on the parameters of the model, and can be maximized for certain combinations of them. Moreover, in order that the coupled ratchets make useful work, the self-correlation time τ must overcome a certain threshold value.

In Sec. II we sketch the main features of the model and of its mean-field analysis (discussed extensively in Ref. [18]) and the way it has to be modified to account for finite τ. In Sec. III we discuss our numerical mean-field results with regard to the phase diagram, stationary probability distribution function (PDF), hysteretic behavior, and the energetics of the process. Finally, in Sec. IV we give our conclusions.

II. THE MODEL AND ITS MEAN-FIELD ANALYSIS

A. The model

As in Ref. [18], we consider the following system of N *globally* coupled stochastic differential equations (interpreted in the Stratonovich sense) for the phases $X_i(t) \in [-L/2, L/2]$ [17]:

$$\dot{X}_i = \left[-\frac{\partial U_i}{\partial X_i} - \frac{1}{N} \sum_{j=1}^{N} K(X_i - X_j) \right] + \sqrt{2T}\, \xi_i(t), \qquad (1)$$

where we assume N to be very large (except for numerical simulations, its particular value is unimportant). The term outside the brackets is nothing but a Langevin force, modeling the effect of thermal fluctuations: T represents the temperature of the environment (as in Refs. [17,18] we shall adopt $T=2$ throughout) and the $\xi_i(t)$ are local, additive, Gaussian white noises with zero mean and variance $1[\langle \xi_i(t) \rangle = 0, \langle \xi_i(t) \xi_j(t') \rangle = \delta_{ij} \delta(t-t')]$.

The interesting features in Eq. (1) come from the terms inside the brackets. In terms of the phaselike real variables x,y that run over the range $[-L/2, L/2]$ of the stochastic processes $X_i(t), X_j(t)$, they are the local "pulsating" potentials $U_i(x,t)$ and the interaction-force function $K(x-y) = -K(y-x)$ between phase oscillators. The latter is a *periodic* function of $x-y$, with period L; the former have the form

$$U_i(x,t) = [V(x) - Fx] + W(x) \sqrt{2Q}\, \eta_i(t). \qquad (2)$$

The terms inside the brackets are global and static: a potential $V(x)$ and an eventual "load force" F, which is just a tool for the analysis of the noise-induced ratchet effect. The interesting features in Eq. (2) are the *fluctuating* local terms, in which Gaussian noises $\eta_i(t)$ of a nonthermal origin couple *multiplicatively* (with intensity Q) to the phases $X_i(t)$, through a global function $W(x)$. Both $V(x)$ and $W(x)$ are *periodic* functions (with period L), and moreover they are *symmetric*: $[V(-x) = V(x), W(-x) = W(x)]$, which means that there is no *built-in* ratchet effect.

At variance with our former work [18], we now assume that the $\eta_i(t)$ are Ornstein-Uhlenbeck:

$$\langle \eta_i(t) \rangle = 0, \ \langle \eta_i(t)\, \eta_j(t') \rangle = \frac{1}{\tau} \delta_{ij} \exp(-|t-t'|/\tau). \quad (3)$$

Following Ref. [17] we adopt $L = 2\pi$ and

$$V(x) = W(x) = -\cos x - A \cos 2x \quad \text{with} \quad A = 0.15, \quad (4)$$

$$K(x) = K_0 \sin x \quad \text{with} \quad K_0 > 0. \qquad (5)$$

As discussed in Ref. [18], when $A>0$ in Eq. (4), the direction of the particle current $\langle \dot{X} \rangle$ is *opposite* to that of symmetry breaking in the stationary probability distribution $P^{st}(x)$ (see Sec. II C for the definition of these magnitudes), which leads in turn to *negative zero-bias conductance* and *anomalous hysteresis*. With the choice in Eq. (5), the second term in Eq. (1) can be cast as $K_0[C_i(t) \sin X_i - S_i(t) \cos X_i]$, with $C_i(t) \equiv N^{-1} \Sigma_j \cos x_j(t)$ and $S_i(t) \equiv N^{-1} \Sigma_j \sin x_j(t)$.

Besides τ, the important parameters in the model just set up are K_0 (governing mostly the "drift" terms in this set of generalized Langevin equations), and Q (governing mostly the "diffusion" ones). For $A \to 0$, this model can be visualized as a set of overdamped pendulums (only their phases matter, not their locations) interacting with one another through a force proportional to the sine of their phase difference (this force is always attractive in the reduced interval $-\pi \leqslant x-y \leqslant \pi$).

B. The approximations

1. Mean-field approximation

In Ref. [18]—the Gaussian stochastic variables $\eta_i(t)$ and $\eta_i(t')$ being *independent* for $t' \neq t$—one could simply add (for each t) $\xi_i(t)$ to $\eta_i(t)$, and regard the $\eta_i(t)$ as *effective* multiplicative Gaussian noises. Equation (1) was then approximated (for $N \to \infty$) in the manner of Curie-Weiss, replacing $C_i(t)$ and $S_i(t)$ by new parameters C_m and S_m, respectively—determined as usual by self-consistency—so decoupling the system of stochastic differential equations (SDE). We thus obtained within this MFA a *Markovian* SDE for the single stochastic process $X(t)$ [19]:

$$\dot{X} = f(X; C_m, S_m) + g(X)\, \eta(t), \qquad (6)$$

where $g(x) = \sqrt{2[T + Q(W')^2]}$ and $f(x; C_m, S_m) = -V'(x) + F - K_0(C_m \sin x - S_m \cos x)$. The associated Fokker-Planck equation (FPE) for the (one-time) PDF $P(x,t; C_m, S_m)$ was

$$\partial_t P = \partial_x\{-[f(x)+\tfrac{1}{2}g(x)\,g'(x)]P\}+\tfrac{1}{2}\partial_{xx}[g^2(x)P]. \tag{7}$$

This can always be cast as a continuity equation $\partial_t P+\partial_x J=0$, so that in the stationary case $\partial_t P=0$ it is $J(x,t;C_m,S_m)=\text{const}=J(C_m,S_m)$.

2. Unified colored-noise approximation

In the present case, neither can we lump $\xi_i(t)$ and $\eta_i(t)$ together nor do we retrieve in the MFA a Markovian SDE. The equivalent of Eq. (6) is now the following system:

$$\dot{X}=f(X;C_m,S_m)+G(X)\;\eta(t)+\sqrt{2T}\,\xi(t),$$

$$\tau\dot{\eta}=-\eta(t)+\zeta(t), \tag{8}$$

which yields a Markovian process in an extended (X,η) space, but not in X space. In Eq. (8) $f(x;C_m,S_m)$ is the same as before, $G(x)=\sqrt{2Q}W'(x)$, and $\zeta(t)$ is another white noise:

$$\langle\zeta(t)\rangle=0,\quad \langle\zeta(t)\zeta(t')\rangle=\delta(t-t'),\quad \langle\zeta(t)\xi(t')\rangle=0.$$

For non-Markovian processes, a FPE can at most result from some (nonsystematic) approximation, e.g., the truncation of a short-τ expansion. Fortunately, under certain conditions a *consistent* Markovian approximation [called ''unified colored-noise approximation'' (UCNA)] can be performed [20]. A long calculation involving path integrals [21] shows that in the $Q\gg T$ regime one can still use Eq. (6) [and hence Eq. (7), as if $X(t)$ were a Markovian process], with new functions that keep information on τ:

$$f(x;C_m,S_m,\tau)=f(x;C_m,S_m)/h(x;C_m,S_m,\tau)$$

and

$$g(x;C_m,S_m,\tau)=g(x)/h(x;C_m,S_m,\tau),$$

where

$$h(x;C_m,S_m,\tau)=1-\tau g(x)[f(x;C_m,S_m)/g(x)]'$$

(the prime stands for the derivative with respect to x).

The UCNA becomes exact not only as $\tau\to 0$, but also for $\tau\to\infty$ [20]. For finite τ, the behavior of $f(x;C_m,S_m,\tau)$ and $g(x;C_m,S_m,\tau)$ depends on $[f(x;C_m,S_m)/g(x)]'$; in some cases (though not in the present work) they can even become singular, and one must resort to interpolation methods to retrieve meaningful results [16,22].

C. Relevant magnitudes

1. The stationary PDF

The normalized stationary solution of Eq. (7) *with periodic boundary conditions* and current density $J(C_m,S_m,\tau)\neq 0$ is

$$P^{st}(x;C_m,S_m,\tau)=\frac{e^{-\phi(x;C_m,S_m,\tau)}\,H(x;C_m,S_m,\tau)}{\mathcal{N}(C_m,S_m,\tau)\,g(x;C_m,S_m,\tau)}, \tag{9}$$

where

$$\phi(x;C_m,S_m,\tau)=-2\int_0^x dy\,\frac{f(y;C_m,S_m,\tau)}{g^2(y;C_m,S_m,\tau)},$$

$$H(x;C_m,S_m,\tau)=\int_x^{x+L} dy\,\frac{\exp[\,\phi(y;C_m,S_m,\tau)]}{g(y;C_m,S_m,\tau)},$$

and $\mathcal{N}(C_m,S_m,\tau)$ is a normalization constant. Although $f(x;C_m,S_m,\tau)$, $g(x;C_m,S_m,\tau)$, and $P^{st}(x;C_m,S_m,\tau)$ are periodic by construction, $\phi(x;C_m,S_m,\tau)$ increases in each cycle by a constant amount [18]. Note also that $P^{st}(x;C_m,S_m,\tau)\geqslant 0$ requires $g(x;C_m,S_m,\tau)>0$, which is a further test for the adequacy of the UCNA.

In the appendix of Ref. [18] it is shown that

$$J(C_m,S_m,\tau)=\frac{1-e^{\phi(L;C_m,S_m,\tau)}}{2\mathcal{N}(C_m,S_m,\tau)}, \tag{10}$$

hence the sign of J is that of $1-e^{\phi(L)}$ and—on the other hand—the ''holonomy'' condition $e^{\phi(L)}=1$ implies $J=0$ and $H(x;C_m,S_m,\tau)=\text{const}=H(C_m,S_m,\tau)$. Equation (10) is a self-consistency relation since both $\mathcal{N}$ and $\phi(L)$ keep information on the shape of $P^{st}(x)$ through C_m and S_m. A nonzero J is always associated with a symmetry breakdown in $P^{st}(x)$ [namely, $P^{st}(-x)\neq P^{st}(x)$]. This may be either *induced* by a nonzero F or *spontaneous* (our main concern here).

2. The particle current

The appearance of a ratchet effect amounts to the existence of a nonvanishing drift term $\langle\dot{X}\rangle$ in the stationary state, in the absence of any forcing ($F=0$). The cause of this spontaneous particle current (the pendulums become rotators in an average sense) is the noise-induced asymmetry in $P^{st}(x)$ [17].

As it is shown in the appendix of Ref. [18],

$$\langle\dot{X}\rangle=\int_{-L/2}^{L/2}dx\,P^{st}(x;C_m,S_m,\tau)[f(x;C_m,S_m,\tau)+\tfrac{1}{2}g(x;C_m,S_m,\tau)g'(x;C_m,S_m,\tau)], \tag{11}$$

which after some calculation yields

$$\langle\dot{X}\rangle=L\left\{\frac{1-e^{\phi(L)}}{2\mathcal{N}}\right\}=L\,J, \tag{12}$$

hence $\langle\dot{X}\rangle$ has the sign of J and, being a measurable quantity, will be regarded as the order parameter in what follows.

3. Energetics of the process

Following Ref. [23], we shall analyze the energetics of the process in terms of the following (specific, i.e., per particle) magnitudes:

(a) $\dot{E}_{in}=\langle \dot{X}\, G(X)\, \eta(t)\rangle=(2Q/\tau)\langle (W')^2\rangle$. Power delivered to the system by the external fluctuations, as obtained from Eqs. (8).

(b) $\dot{E}_{out}=-\langle \dot{X}\rangle F$. Power delivered by the system against the force F.

From these we may calculate the efficiency $\varepsilon=\dot{E}_{out}/\dot{E}_{in}$ of the mechanical rectifying process and (since the internal energy of the system is constant in the stationary regime) the dissipated power $q=\dot{E}_{in}-\dot{E}_{out}$, as well as the entropy production $\dot{S}=q/T$ per particle.

D. Relevant equations

1. The self-consistency equations

As stated before, the values of S_m and C_m arise from requiring self-consistency, which amounts to solving (for given Q, K_0, F, and τ) the system of nonlinear integral equations

$$F_{cm}(C_m,S_m,\tau)=C_m, \tag{13}$$

$$F_{sm}(C_m,S_m,\tau)=S_m, \tag{14}$$

where

$$F_{cm}(C_m,S_m,\tau)\equiv\langle\cos x\rangle=\int_{-L/2}^{L/2}dx\,\cos x P^{st}(x;C_m,S_m,\tau),$$

$$F_{sm}(C_m,S_m,\tau)\equiv\langle\sin x\rangle=\int_{-L/2}^{L/2}dx\,\sin x P^{st}(x;C_m,S_m,\tau).$$

These equations give

$$C_m(Q,K_0,F,\tau) \quad \text{and} \quad S_m(Q,K_0,F,\tau)$$

for each set of the parameters that define the state of the system.

For $F=0$ there are always one or more solutions to Eqs. (13) and (14) with $S_m=0$, and one of them is the stable one in the ''disordered'' phase [in this case $P^{st}(x)$ is an even function of x]. So the problem of self-consistency reduces to the numerical search of solutions to Eq. (13), with $S_m=0$ (what in Ref. [18] we have called ''homogeneous solutions''). Since $\cos x$ in this equation is an even function of x, in order to determine the stability of these solutions it suffices to use the Curie-Weiss (one-parameter) criterion, i.e., to check whether the slope of F_{sm} at $S_m=0$ is <1 or >1.

As argued in Ref. [17], for $N\to\infty$ a noise-induced nonequilibrium transition takes place *generically* towards an ''ordered'' phase where $P^{st}(-x)\neq P^{st}(x)$. In the present scheme this asymmetry should be evidenced by the fact that the solution with $S_m=0$ becomes unstable in favor of other two solutions such that $P_2^{st}(x)=P_1^{st}(-x)$, characterized by *nonzero* values $\pm|S_m|$ (this fact confers also S_m the rank of an order parameter, but we shall use $\langle\dot{X}\rangle$ to that end). Nonetheless, even in the ordered phase the ''homogeneous'' solutions are of interest [this time as a secure starting guess for the Newton-Raphson solution of Eqs. (13) and (14), given the fact that some solutions may suddenly disappear].

2. The phase boundary

Equation (14) proves impractical for the task of finding the curve that separates the ordered phase from the disordered one, since on that curve S_m is still zero. For that goal (exclusively), we solve, instead of Eqs. (13) and (14), the following system:

$$\int_{-L/2}^{L/2}dx\,\cos x P^{st}(x;C_m,0,\tau)=C_m, \tag{15}$$

$$\int_{-L/2}^{L/2}dx\,\sin x\frac{\partial}{\partial S_m}P^{st}(x;C_m,S_m,\tau)\big|_{S_m=0}=1. \tag{16}$$

III. NUMERICAL MEAN-FIELD RESULTS

A. K_0 vs Q phase diagram

1. Summary of the $\tau=0$ results

In Ref. [18]—besides obtaining within the MFA a phase boundary that fully coincided with that (numerical) in Fig. 1(b) of Ref. [17]—we have shown that a transition takes place inside the ordered phase, in the behavior of the system.

(1) For K_0/Q large enough (''interaction-driven regime'' or IDR) the system typically exhibits an *anomalous* (namely, clockwise) hysteresis cycle in its $\langle\dot{X}\rangle$ vs F characteristic, and *unimodal* stationary PDF.

(2) For lower values of K_0/Q (''noise-driven regime'' or NDR) the $\langle\dot{X}\rangle$ vs F characteristic shows *normal* (counterclockwise) hysteresis and the PDF becomes *bimodal*, remaining so as Q increases (or K_0 decreases) further. As the disordered region is reentered the PDF becomes symmetric again, the peak at π being then higher than that at 0 (see Fig. 3 in Ref. [18] and the $\tau=0$ PDF in Fig. 3 of this paper).

A good estimation of the boundary between the IDR and the NDR was provided in Ref. [18] by the line separating two sectors *within the ordered region* with regard to the ''homogeneous'' ($S_m=0$) solutions to the MFA self-consistency equations: below it (NDR), there is *a single* such solution to Eqs. (13) and (14); above it (IDR), there are three, five, etc. This line presented a cusp whose meaning we investigated in Ref. [18] for $\tau=0$, finding a physical feature (i.e., one not attributable to MFA artifacts): whereas the character of the hysteresis loop changed from anomalous to normal in going from the IDR to the NDR to the right of this cusp, it remained anomalous while crossing this line on the left side.

Since the transition from anomalous to normal hysteresis in going from the IDR to the NDR is typically preceded by the disappearance of *pairs* of solutions with $S_m=0$, the line in the phase diagram below which *a single* ''homogeneous'' solution exists (dashed line in Fig. 1 of Ref. [18] and solid *thin* line in Fig. 1 of this paper) *provides an estimation* of the place at which the former transition occurs. Of course both phenomena are different, and so the disappearance of a pair of solutions with $S_m=0$ *does not imply* an anomalous-to-

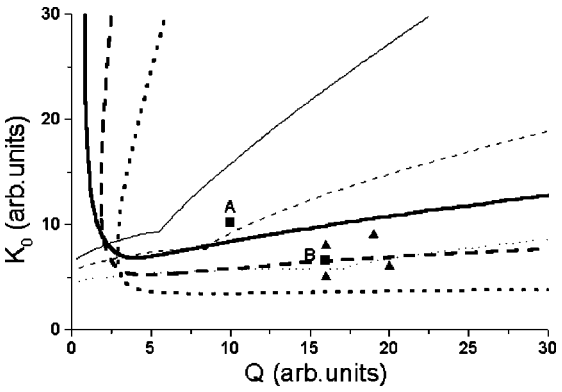

FIG. 1. K_0 vs Q phase diagram of the model for $F=0$. Solid lines, $\tau=0.0$; dashed lines, $\tau=0.1$; dotted lines, $\tau=0.3$. For each value of τ the ordered region lies above and to the right of the corresponding thick line. Above the thin lines there may exist several solutions when $S_m \neq 0$, whereas below them there may exist at most one. Points $A=(10.0,10.2)$ and $B=(16.0,6.6)$ indicate two different regimes at which the transport properties and the shape of $P^{st}(x)$ have been investigated. The triangles are explained in Sec. III C.

normal transition (an example of this assertion is that there was no change in the character of the hysteresis loop at the left of the cusp).

It must be emphasized that $\langle \dot{X} \rangle$ (denoted as V_m in the figures) shows hysteretic behavior as a function of F everywhere inside the ordered phase [24]. In the IDR, the *height* of the (anomalous) hysteresis loop increases continuously at the phase boundary ($\langle \dot{X} \rangle$ acts as an order parameter in a second-order phase transition). Instead, the disappearance of the (normal) hysteresis loop in the NDR proceeds by shrinking its *width* at a more or less finite height (although the transition at the reentrance is of *second* order, it is so steep that it resembles a first order one).

2. The PDF and the hysteresis' character

Here we want to discuss the relation between the PDF and the normal or anomalous character of the hysteresis loop. To reach this goal, we recall that in Ref. [18] we have introduced the idea of an *effective potential* that includes several contributions. First, a term corresponding to the symmetric potential $V(x)=\cos x+2A\cos 2x$, affecting all oscillators. Second, a term that corresponds to the mutual interaction between the oscillators $K_0(C_m \sin x - S_m \cos x)$. And finally, third and fourth terms arising from the load force F, and a symmetric one arising from the Stratonovich prescription to treat the noisy term [yielding a term given by Q times $S(x)S'(x)/2$], respectively.

Anomalous hysteretic behavior. The anomalous hysteresis loop arises in the IDR, the region where the interaction (the second term indicated above) breaks the symmetry of the periodic potential, producing an asymmetric effective potential (that, if linearized, has a sawtooth profile) which, being turned on and off by the noise, produces a flux opposite to the the sign of S_m. In the ordered region the model has two single-peaked solutions: one with $S_m<0$, and another one with $S_m>0$, whose moduli, for $F=0$, are equal. A strong enough F washes out the potential wells eliminating the possibility of stationary solutions and inducing a limit cycle (that, as indicated in Sec. III B 1, has been actually found and will be discussed in detail elsewhere).

However, one of the stationary solutions disappears before the other. Such a solution is the one with the sign S_m opposite to the sign of F (that is, if $F>0$, the one with $S_m<0$ is the first to disappear). Looking at the v_m vs F diagram, for a critical value of F, it is the $v_m>0$ branch that first disappears, while the other survives until another, larger, critical value of F is reached. This produces the anomalous hysteretic behavior.

The relevant question is, clearly, why the branch with the sign of S_m opposite to the one of F disappears first? In order to understand this, we can resort to the coupled pendulums picture (case $A=0$). Each value of S_m corresponds to a position of the pendulum at each side of the symmetry axis. When a load force is applied in a given direction, it reduces one of those angles while increasing the other. For instance, if $F>0$, the angle with $S_m<0$ is reduced and that with $S_m>0$ is increased. As the value of S_m controls the asymmetry of the effective potential (for larger $|S_m|$ it becomes more asymmetric, and for $S_m=0$ it becomes fully symmetric), increasing F we not only wash out the potential wells but in addition reduce the asymmetry of the solution for $S_m<0$ and enhance the one with $S_m>0$. This is the reason why, at a smaller critical value, the solution with $S_m<0$ disappears first. When $F<0$ we have the specular situation.

Normal hysteretic behavior. When the noise intensity Q is very large, it can completely hide the effect of the coupling, and the effective potential becomes symmetric again, with only one stable solution (with $v_m=0$ if $F=0$). For smaller values of Q, but still large enough to dominate the coupling, the solutions show values of S_m that varies only sightly with F. This can again be understood resorting to the coupled pendulums example. We have shown [18] that in the NDR, for each solution ($S_m>0$ and $S_m<0$), the PDF presents two peaks, one near zero and the other near π. For $F>0$, the two angles (or peaks) corresponding to $S_m<0$ approach the symmetry axis (one $\rightarrow 0$ and the other $\rightarrow \pi$), while the corresponding ones for $S_m>0$ depart from the axis. Due to the symmetry of their positions, the mean values corresponding to $S_m<0$ and $S_m>0$ will remain approximately constant. This means that, on one hand, when F grows, the peaks of the PDF for $S_m<0$ separate, while those corresponding to $S_m>0$ tend to coalesce. On the other hand, comparing the form of the effective potential for both solutions ($S_m<0$ and $S_m>0$) for a value of F near the critical one F_c (but, *and only for comparison purposes*, adopting $F=0$), we see that while for $S_m>0$ it is almost symmetrical, for $S_m<0$ remains strongly asymmetrical. It is precisely the first solution ($S_m>0$) that disappears at $F=F_c$. Hence, for Q large enough, and depending on the sign of F, the noise's symmetrizing effect (that for Q extremely large destroys order) is markedly enhanced by one of the solutions (the one where S_m has the same sign as F) and reduced by the other (the one where S_m has a sign opposite to that of F). In the first case (sign of S_m

coincident with the sign of F) a critical value of F ($F=F_c$) exists, such that the effective potential becomes completely symmetrical and the corresponding solution dissappears (corresponding to the branch with $v_m<0$) while the other (corresponding to the branch with $v_m>0$) remains. This is the origin of the normal hysteretic behavior in the NDR.

3. τ-dependence of phase boundary and IDR-NDR transition line

As in Ref. [18]—and as stated in Sec. II A—throughout this work we set $T=2.0$ and $A=0.15$. Our first task is to investigate the effects that a nonzero self-correlation time τ of the multiplicative noises $\eta_i(t)$ produces on the K_0 vs Q phase diagram shown as Fig. 1 in Ref. [18]. Figure 1 is an extension to the $\tau\neq 0$ case of Fig. 1 in Ref. [18], drawn on the same scale; we have nonetheless altered slightly our former conventions: the phase boundary (formerly depicted as a solid line) is now indicated by a *thick* line, whereas the line separating the IDR from the NDR—formerly indicated by a dashed line—is now depicted as a *thin* one.

The most important effect of the multiplicative noises' self-correlation is the appearance (for *any* $\tau\neq 0$) of *reentrant* behavior as *the coupling* K_0 increases for $Q=$const (upper branch of the phase boundary). This (counterintuitive) *disordering* effect of self-correlation in the IDR had already been found in the mean-field analysis of a lattice model displaying a similar (symmetry-breaking) nonequilibrium phase transition, jointly induced by coupling and noise [16]. On the other hand, the lower branch of the phase boundary shifts toward lower K_0 values and the reentrance with respect to Q (characteristic of the $\tau=0$ behavior) tends to disappear as τ increases, which configures an *ordering* effect in the NDR.

The boundary between the NDR and the IDR becomes almost independent of Q as τ increases, and the aforementioned cusp shifts rightwards.

B. τ-dependence of stationary PDF and transport properties at selected points

The τ dependence of quantities such as the stationary PDF, the mobility and the efficiency of the mechanical conversion process can only be studied at selected points in the (Q,K_0) plane [alternatively, one could choose either to vary K_0 at fixed (τ,Q), or Q at fixed (τ,K_0)]. Point A in Fig. 1—with coordinates (10.0,10.2)— lies in the range analyzed in Ref. [18]. Point B—with coordinates (16.0,6.6)—was outside the range of interest for $\tau=0$ but now (as we shall see) deserves due attention.

In a preliminary work [25] we have studied the τ dependence of the stationary PDF and that of the mobility at point A. We include here a brief sketch of the latter results in order to make explicit comparisons between that regime and that corresponding to point B, regarding (a) the complexity of the hysteresis cycle and (b) the efficiency ε of the mechanical rectification process.

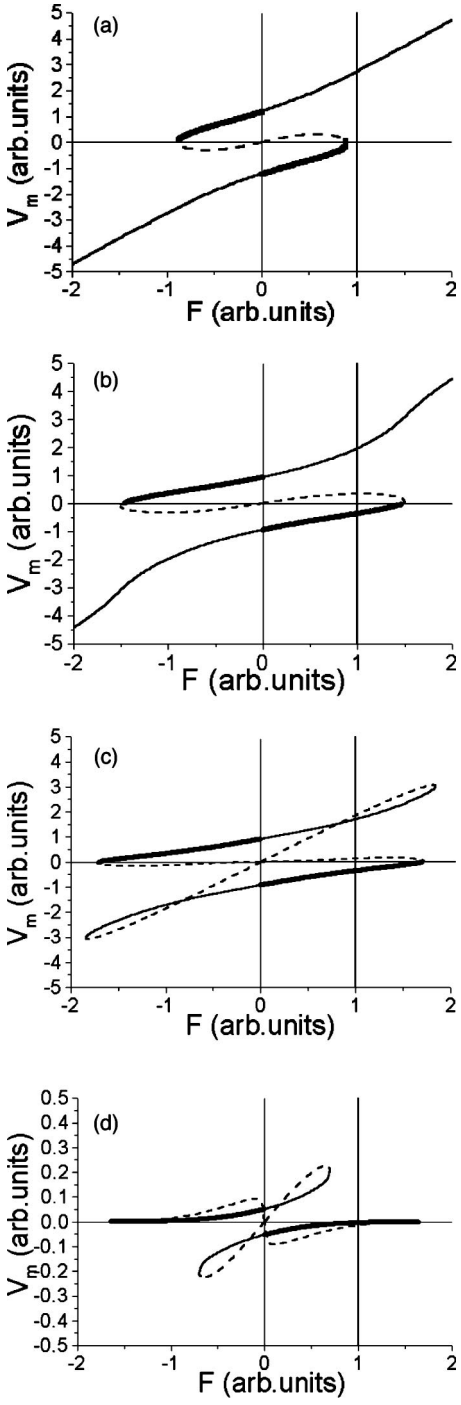

FIG. 2. Evolution with τ of the $V_m\equiv\langle\dot{X}\rangle$ vs F characteristic (in MFA) at point A: (a) $\tau=0.0$; (b) $\tau=0.05$; (c) $\tau=0.1$; (d) $\tau=0.3$. Solid lines, stable branches; dashed lines, unstable branches; thick lines, segments where $\varepsilon>0$. The $F=1$ line has been highlighted. Note the different vertical scale in (d).

1. Summary of features at point A

Figure 2 shows the τ evolution of the $\langle\dot{X}\rangle$ vs F characteristic at point A. In order to facilitate the analysis of the energetics in Sec. III D, we have thickened in Fig. 2 those segments where $\varepsilon>0$ and marked a vertical line at $F=1$.

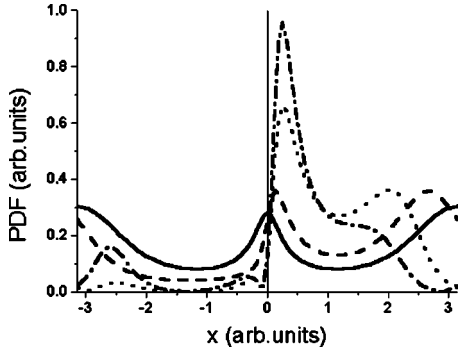

FIG. 3. Shape of the stationary PDF $P^{st}(x)$ at point B, for $F=0.0$ and different values of τ. Solid line, $\tau=0.0$; dashed line, $\tau=0.1$; dotted line, $\tau=0.3$; dot-dashed line, $\tau=1.0$. Each asymmetric PDF has its own reflected partner $P^{st}(-x)$, not shown.

The transition from normal to anomalous hysteresis occurs at this point for a value of τ such that the F dominions of both stable curves coincide.

The main feature is the existence in the IDR [cases (c) and (d)] of *multiple* unstable branches, characterized by different sets of S_m and C_m (and generically by different values of $\langle \dot{X} \rangle$) for each value of F. We have depicted only two of them: those joining the stable branches, giving an altogether closed curve in the $(F,\langle \dot{X} \rangle)$ plane (the crossings are simply a projection effect). There is a third unstable branch not joining any stable one, and hence not relevant for the analysis of the hysteresis cycle. This unstable branch is not completely irrelevant, however, since it extends beyond the range of F for which stable solutions exist [cases (c) and (d)], indicating the possible existence of a limit cycle that, at variance with the result of [26], was actually found within a mean-field scheme. Details about the characteristics of such a limit cycle will be published elsewhere.

Another important feature is that one unstable branch always joins the stable ones at $\langle \dot{X} \rangle = 0$ (we shall see the consequences of this in Sec. III D).

2. Analysis at point B

As Fig. 1 shows, this point lies well inside the *disordered* region for $\tau=0$, bordering the NDR for $\tau=0.1$, and just inside the IDR for $\tau=0.3$. Hence not only the NDR-IDR transition, but also the ordering phase transition can be monitored for point B as τ increases. Note moreover that for $\tau=0.3$, this point is located *to the left* of the aforementioned cusp in the boundary between the IDR and the NDR.

Figure 3 illustrates the evolution in the shape of the stationary mean-field PDF as τ increases. For $\tau=0$ it is symmetric and (as stated before) has peaks at $x=0$ and $x=\pi$, the latter being higher than the former. For $\tau=0.1$ symmetry breakdown has occurred and two stable solutions of Eqs. (13) and (14) with $S_m \neq 0$ have appeared, which are such that $P_2^{st}(x)=P_1^{st}(-x)$. In each of them we can see a depletion of probability for x having one sign, in favor of the other. In particular, the peak formerly at $x=\pi$ shifts towards lesser values of $|x|$ and its height is roughly equal to that of the peak formerly at $x=0$ (which has also shifted a little). For $\tau=0.3$ the PDF is still bimodal but the depletion of one region is significative and the peak near $x=0$ dominates. For $\tau=1.0$ the PDF has already become unimodal.

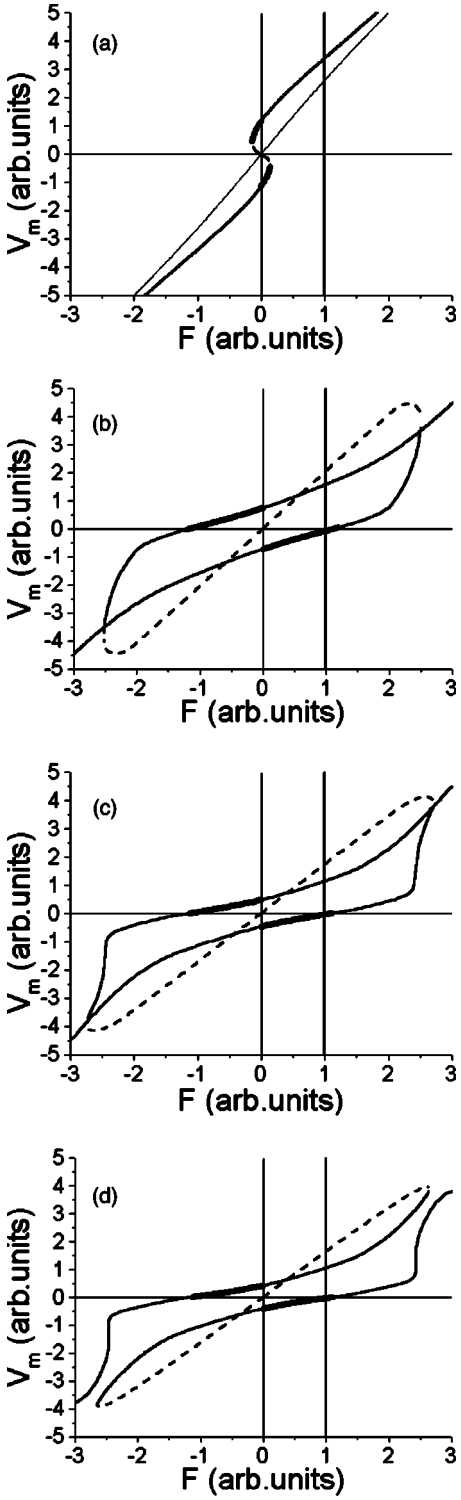

FIG. 4. Evolution with τ of the $\langle \dot{X} \rangle$ vs F characteristic (in MFA) at point B: (a) $\tau=0.0$ and 0.1; (b) $\tau=0.3$; (c) $\tau=0.375$; (d) $\tau=0.4$. Solid lines, stable branches; dashed lines, unstable branches.

Figure 4 follows the τ evolution of the $\langle \dot{X} \rangle$ vs F characteristic obtained in the MFA. The sequence is in some sense

inverse to that shown in Fig. 7 of Ref. [18] since as τ increases, the point enters the ordered phase ''from the left'' (i.e., from the reentrant boundary). Contrary to what happens in the vicinity of the upper branch of the phase boundary (see, e.g., Fig. 6 in Ref. [18]) the ''susceptibility'' or zero-bias conductance (in the unbroken-symmetry phase) is *positive* in the vicinity of this branch [$\tau=0$ curve in Fig. 4(a)]. At $\tau=0.1$ [also in Fig. 4(a)] we see a small (normal) hysteresis loop that—together with the symmetry breakdown in the PDF—indicates that the system is already in the ordered phase (a fact not totally evident in Fig. 1). The pattern resembles that shown in Fig. 2(a) (for point A at $\tau=0$) in that only *one* unstable branch (the only one existing in the IDR) joins the stable ones. There is, however, an important difference: since the slope of the unstable branch in the $(F,\langle\dot{X}\rangle)$ plane is negative in this case, it can have *positive* efficiency [a fact observed in Figs. 6(d) and 8(a) and 8(b) for $F=1$].

The mechanism whereby the hysteresis cycle reverses its sense at point *B* is however very different from that at point *A*. For larger values of τ [see in Fig. 4(b) the situation at $\tau=0.3$] the mean-field characteristic becomes more and more kinky, and the projections of its stable branches cross. However, at $\tau=0.375$, *real* stable branch crossings occur [Fig. 4(c)] (at $F=\pm 2.88,\langle\dot{X}\rangle=\pm 4.223\,35$, both stable branches have $C_m=\pm 0.150\,88, S_m=\pm 0.285\,19$). Thus—as τ increases further—the relevant unstable branch (from a total of three) detaches from the stable branches it was attached to for lower τ, and reattaches to the other ones. The hysteresis loop thus reverses its cycle [as can be seen for $\tau=0.4$ in Fig. 4(d)] and becomes anomalous (a behavior typical of the IDR), but the reason here is simply that the ''upper'' and ''lower'' stable branches have exchanged their roles.

C. The character of the transition around the cusp and the complexity of the hysteresis cycle

In Ref. [18], the following feature was observed for $\tau=0$: whereas at the right of the cusp the character of the hysteresis cycle changes from anomalous to normal in going from the IDR to the NDR, on the left side the cycle remains anomalous. This is also the pattern for τ not too large (say, 0.1). For $\tau\geqslant 0.3$ instead, an anomalous-to-normal transition takes place at both sides of the cusp. In Fig. 5 we exhibit—for $\tau=0.3$ [see in Fig. 4(b) the situation at point B]—the $\langle\dot{X}\rangle$ vs F characteristic at the points marked with triangles in Fig. 1. There is a pair of such points at each side of the cusp in the thin dotted line of Fig. 1. For each pair, one point lies in the NDR [Figs. 5(a) and 5(c)] and the other in the IDR [Figs. 5(b) and 5(d)]. Note the different scales at both regimes.

Another feature [already apparent in Figs. 4(c) and 4(d), but that becomes evident in Figs. 5(b) and 5(d)] is the higher complexity in the shape of the stable branches in the IDR, for $\tau\geqslant 0.3$. It is associated to the arising of five or more homogeneous solutions to the mean-field equations in the IDR. As these aspects could be a spurious result due to the mean-field scheme, we are presently undertaking the numerical simulation in this regime in order to confirm or reject the features predicted by the mean-field treatment. Such results will be published elsewhere.

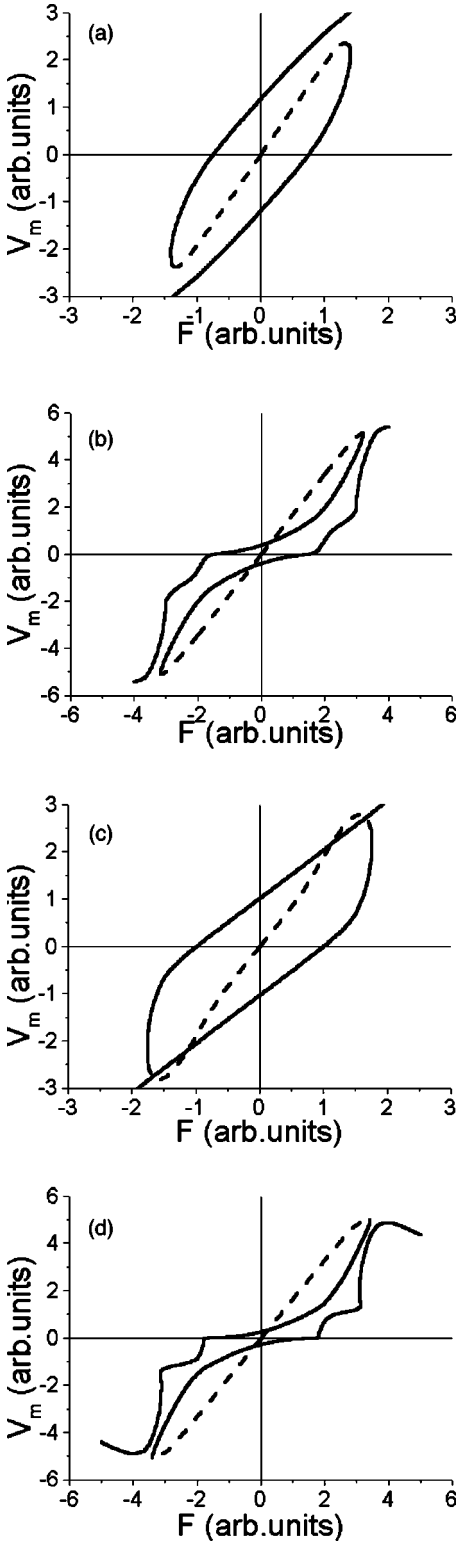

FIG. 5. $\langle\dot{X}\rangle$ vs F characteristic (in MFA) around point B, for $\tau=0.3$. Solid lines, stable branches; dashed lines, unstable branches. (a) $Q=16.0, K_0=5.0$; (b) $Q=16.0, K_0=8.0$; (c) $Q=20.0, K_0=6.0$; (d) $Q=19.0, K_0=9.0$.

D. Energetics

Figure 6 shows the efficiency ε— defined in Sec. II C 3—as a function of F, at point *A* (in correspondence with Fig. 2,

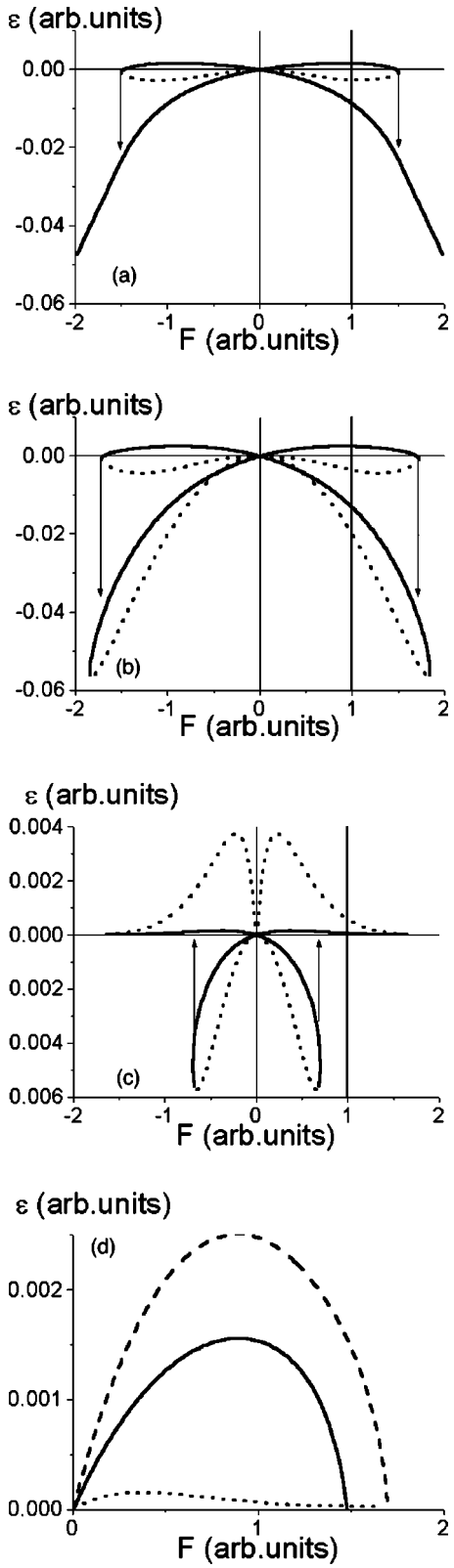

FIG. 6. Efficiency ε as a function of F, at point A. (a) $\tau=0.05$; (b) $\tau=0.1$; (c) $\tau=0.3$ [solid lines, stable branches; dotted lines, unstable branches; note the different scale of (c)]. (d) $\varepsilon>0$ region of the stable branches (solid line, $\tau=0.05$; dashed line, $\tau=0.1$; dotted line, $\tau=0.3$).

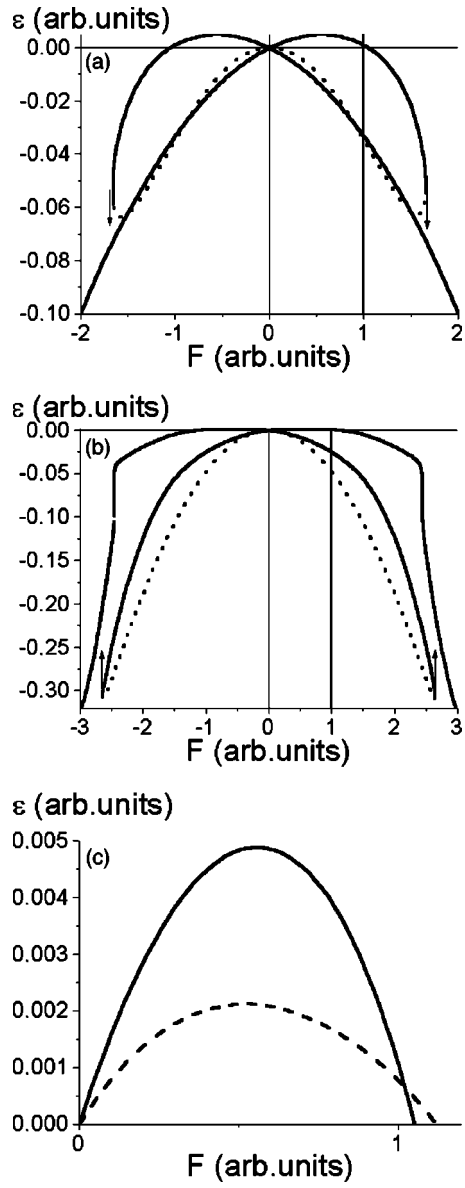

FIG. 7. Efficiency ε as a function of F, at point B. (a) $\tau=0.2$; (b) $\tau=0.4$ [solid lines, stable branches; dotted lines, unstable branches]; (c) $\varepsilon>0$ region of the stable branches (solid line, $\tau=0.2$; dashed line, $\tau=0.4$).

where we have thickened the ranges where $\varepsilon>0$). For the-sake of completeness, we have also plotted ε vs F at point B (Fig. 7, corresponding to Fig. 4).

Before we delve in the separate analysis of each such regime, we shall comment on some general features. As Figs. 6 and 7 show, for each value of τ there is an optimal value of $|F|$ yielding the maximum efficiency. Moreover, Figs. 6(d) and 7(c) tell us that the maximum expectable efficiency is of the order of 10^{-3}.

Figures 6(a) and 6(b) derive respectively from Figs. 2(b) and 2(c), where the $\langle \dot{X} \rangle$ vs F hysteresis cycle is normal. In the regions where the F dominions do not overlap, the stable branch in Fig. 2 has the sign of F; so $\varepsilon<0$ until F is reverted. Then ε becomes positive attaining a maximum value, and vanishes exactly where the jump to the other stable

branch (having a strongly negative efficiency) occurs. Moreover, the open or closed character of the lower branch can be traced back to the (open or closed) character of the $\langle \dot{X} \rangle$ vs F characteristic, namely, to the existence of a single or multiple unstable branches.

Figure 6(c) corresponds to Fig. 2(d), where the $\langle \dot{X} \rangle$ vs F hysteresis cycle is anomalous. A remarkable feature of this case is that it is the *unstable* branch that has a positive efficiency of the order of 10^{-3} [dotted line in Fig. 6(c)] whereas the maximum positive efficiency for the stable one is of the order of 10^{-4} [solid line in Fig. 6(c) and dotted line in Fig. 6(d)]. Here—in the regions where the F dominions do not overlap—the stable branch in Fig. 2 has opposite sign to F; so $\varepsilon > 0$ (albeit very small) until F is reverted. Then ε becomes negative until it joins the second unstable branch, and suddenly jumps from a negative value to a (very small) positive value.

With regard to point B, the value of τ in Fig. 7(a) is intermediate between those of Figs. 4(a) and 4(b), and corresponds to a normal hysteresis cycle. The one in Fig. 7(b) is that of the anomalous hysteresis cycle shown in Fig. 4(d). In both cases, the transition between stable branches does not have an associated jump in ε (from the point of view of the efficiency the transition is less abrupt, since it occurs between close negative values of ε).

Although the noise strength Q and self-correlation time τ (as well as the global coupling K_0) are not control parameters—as is the tilt F of the potential—it is nonetheless interesting to study how the efficiency ε of the mechanical rectification process depends on them. Thus we have plotted—for $F = 1.0$, highlighted in Figs. 2 and 4—ε as a function of τ, at points A [Figs. 8(a) and 8(b)] and B [Figs. 8(c) and 8(d)].

In both cases, the shape of the curve is that of a normal hysteresis cycle. The stable branch starting at $\tau = 0.0$ disappears—through a bifurcation resembling an inverse saddle-node one—at a finite value of τ_i (0.22 for point A and 0.88 for point B), and has $\varepsilon < 0$ throughout. On the other hand, a direct bifurcation occurring at a *finite* value τ_d (0.01 for point A and 0.17 for point B) gives rise to a new stable branch having $\varepsilon > 0$ (at $F = 1$) for $\tau > \tau_d$. For $\tau > \tau_i$, only the second branch remains. These plots can be understood by recalling Figs. 2 and 4, respectively—namely, the $V_m \equiv \langle \dot{X} \rangle$ vs F plots for τ, Q, and K_0 fixed—in the vicinity of $F = 1$.

In the NDR—wherein the cycle is normal—the $\langle \dot{X} \rangle$ vs F characteristic exhibits two stable branches and an unstable one, forming both inverse (for $F > 0$) and direct (for $F < 0$) bifurcations. Both move towards $F = 0$ as τ decreases (the width of the hysteresis loop diminishes). For some value of τ the inverse bifurcation crosses the $F = 1$ line, in coincidence with the direct one in Fig. 8 (ε vs τ plot).

On the other hand—again observing Figs. 2 and 4—an anomalous-to-normal hysteresis transition occurs as τ increases. The bifurcations are exchanged: the inverse one corresponds to $F < 0$ and the direct one to $F > 0$. Since these bifurcations move towards $F = 0$ as τ increases, the $F > 0$ one gives rise to the inverse bifurcation in Fig. 8 for $F = 1$.

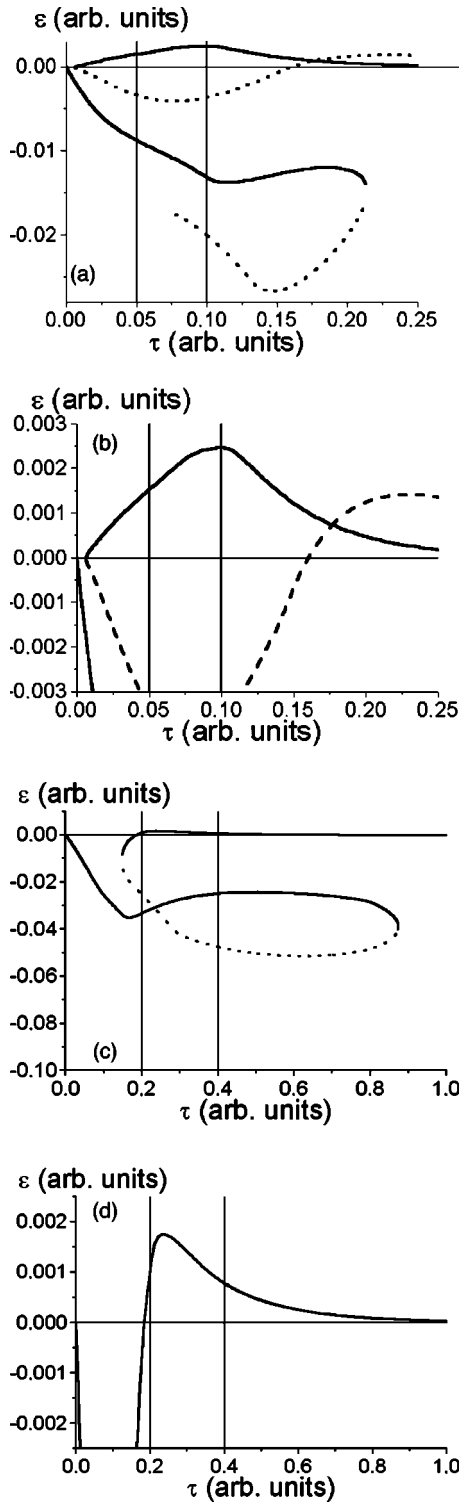

FIG. 8. Efficiency ε as a function of τ, for $F = 1.0$: (a) at point A; (b) detail of (a); (c) at point B; (d) detail of (c).

IV. CONCLUSIONS

In this paper, we have analyzed—within the MFA—the consequences of the $\eta_i(t)$ in Eq. (2) being *Ornstein-Uhlenbeck* noises, with common strength Q and self-correlation time τ. Equation (2), together with Eqs. (1), (4), and (5) constitute the model set up in Ref. [17], whose mean-

field analysis for $\tau=0$ was thoroughly worked out in Refs. [17,18].

(1) Consistent with the conclusions of a similar analysis undertaken in Refs. [16] for a lattice model, we observe a reentrance in the phase diagram as a function of K_0, not present for $\tau=0$ (increasing the coupling beyond some value, the system gets *disordered* again). On the other hand, in the (NDR) there is an *ordering* effect, since the trend as τ increases is to ''wash out'' the reentrance as a function of Q.

(2) The line below which *a single* ''homogeneous'' ($S_m=0$) solution exists to the MFA self-consistency equations [Eqs. (13) and (14)] (an MFA indicator of the IDR-NDR transition) shifts toward lower K_0 values and flattens; at the same time, its characteristic cusp shifts toward larger Q values.

(3) Color affects severely the response of the particle current to the bias force. As τ increases, there appear new solutions to the mean-field equations in the IDR, leading to a more complex (anomalous) hysteretic behavior in the $\langle \dot{X} \rangle$ vs F characteristic.

(4) $\langle \dot{X} \rangle$ also exhibits (anomalous or normal, depending on the case) hysteretic behavior with respect to Q, K_0, or τ, provided that the range on which that parameter is varied goes through the anomalous-normal hysteresis transition in the $\langle \dot{X} \rangle$ vs F characteristic.

(5) The efficiency ε of the mechanical rectification process depends strongly on the parameters of the model, and can be maximized for certain combinations of them. In particular—given Q, K_0, and $|F|$—there is an optimum self-correlation time of the flashing potentials.

(6) In the regimes analyzed in this paper, it is impossible to have $\varepsilon>0$ if the multiplicative noises are white. In order that the coupled ratchets make useful work, the self-correlation time τ must overcome a certain threshold value.

ACKNOWLEDGMENTS

The authors thank R. Toral for enlightening suggestions and V. Grunfeld for a critical reading of the manuscript. S.E.M. acknowledges support from CONICET, and H.S.W. acknowledges support from CONICET and ANPCyT (both Argentinian agencies).

[1] W. Horsthemke and R. Lefever, *Noise-Induced Transitions: Theory and Applications in Physics, Chemistry and Biology* (Springer-Verlag, Berlin, 1984).

[2] C. Meunier and A.D. Verga, J. Stat. Phys. **50**, 345 (1988); H. Zeghlache, P. Mandel, and C. Van den Broeck, Phys. Rev. A **40**, 286 (1989); R. C. Buceta and E. Tirapegui, in *Instabilities and Nonequilibrium Structures III*, edited by E. Tirapegui and W. Zeller (Kluwer, Dordrecht, 1991), p. 171.

[3] L. Gammaitoni, P. Hänggi, P. Jung, and F. Marchesoni, Rev. Mod. Phys. **70**, 223 (1998).

[4] H.S. Wio, Phys. Rev. E **54**, R3075 (1996); F. Castelpoggi and H.S. Wio, Europhys. Lett. **38**, 91 (1997); S. Bouzat and H.S. Wio, Phys. Rev. E **59**, 5142 (1999); B. von Haeften, R. Deza, and H.S. Wio, Phys. Rev. Lett. **84**, 404 (2000).

[5] N.V. Agudov, Phys. Rev. E **57**, 2618 (1998).

[6] J. García-Ojalvo and J. M. Sancho, *Noise in Spatially Extended Systems* (Springer-Verlag, Berlin, 1999).

[7] C. Van den Broeck, J.M.R. Parrondo, and R. Toral, Phys. Rev. Lett. **73**, 3395 (1994); C. Van den Broeck, J.M.R. Parrondo, R. Toral, and R. Kawai, Phys. Rev. E **55**, 4084 (1997).

[8] P. Reimann, Phys. Rep. **361**, 57 (2002).

[9] R. P. Feynman, R. B. Leighton, and M. Sands, *The Feynman Lectures on Physics, Mainly Mechanics, Radiation, and Heat*, (Addison-Wesley, Reading, MA, 1966), Vol. I, Chap. 46.

[10] D. Astumian, Sci. Am. **285** (2), 45 (2001); M. Rourkes, *ibid.* **285** (3), 42 (2001); G.M. Whitesides, *ibid.* **285** (3), 70 (2001).

[11] A.V. Soldatov, Mod. Phys. Lett. B **7**, 1253 (1993).

[12] J. M. Sancho and M. San Miguel, in *Noise in Nonlinear Dynamical Systems*, edited by F. Moss and P. V. E. McClintock (Cambridge U. Press, Cambridge, 1989), p. 72.

[13] M. Dykman and K. Lindenberg, in *Some Problems in Statistical Physics*, edited by G. Weiss (SIAM, Philadelphia, 1993), p. 41.

[14] P. Hänggi and P. Jung, in *Advances in Chemical Physics*, edited by I. Prigogine and S. A. Rice (Wiley, New York, 1995), Vol. LXXXIX, p. 239.

[15] F. Castro, A.D. Sánchez, and H.S. Wio, Phys. Rev. Lett. **75**, 1691 (1995).

[16] S. Mangioni, R. Deza, H.S. Wio, and R. Toral, Phys. Rev. Lett. **79**, 2389 (1997); S. Mangioni, R. Deza, R. Toral, and H.S. Wio, Phys. Rev. E **61**, 223 (2000).

[17] P. Reimann, R. Kawai, C. Van den Broeck, and P. Hänggi, Europhys. Lett. **45**, 545 (1999).

[18] S. Mangioni, R. Deza, and H.S. Wio, Phys. Rev. E **63**, 041115 (2001).

[19] A SDE is called *Markovian* if its solution is a Markovian stochastic process; for the definition of the latter see N. G. Van Kampen, *Stochastic Processes in Physics and Chemistry* (North-Holland, Amsterdam, 1982); C. W. Gardiner, *Handbook of Stochastic Methods for Physics, Chemistry and the Natural Sciences*, 2nd ed. (Springer-Verlag, Berlin, 1985); H. Risken, *The Fokker-Planck Equation: Methods of Solution and Applications*, 2nd ed. (Springer-Verlag, Berlin, 1989); H. S. Wio, *An Introduction to Stochastic Processes and Nonequilibrium Statistical Physics* (World Scientific, Singapore, 1995).

[20] P. Jung and P. Hänggi, Phys. Rev. A **35**, 4464 (1987); A.J.R. Madureira, P. Hänggi, V. Buonomano, and W.A. Rodrigues, Phys. Rev. E **51**, 3849 (1995).

[21] P. Colet, H.S. Wio, and M. San Miguel, Phys. Rev. A **39**, 6094 (1989); H.S. Wio, P. Colet, M. San Miguel, L. Pesquera, and M.A. Rodríguez, *ibid.* **40**, 7312 (1989).

[22] F. Castro, H.S. Wio, and G. Abramson, Phys. Rev. E **52**, 159 (1995).

[23] J. Buceta, J.M. Parrondo, C. Van den Broeck, and F.J. de la Rubia, Phys. Rev. E **61**, 6287 (2000).

[24] By continuity, one must expect hysteretic behavior as a function of either K_0 or Q, fixing $F \neq 0$ and the remaining parameter.

[25] H. S. Wio, S. Mangioni, and R. Deza, *Proceedings of the IX Latin American Workshop on Nonlinear Physics* (Cocoyoc, Mexico, 2001); Physica D **168-169**, 186-194 (2002).

[26] M. Kostur, J. Luczka, and L. Schimansky-Geier, Phys. Rev. E **65**, 051115 (2002).